Journal of Scientific and Innovative Research 2017; 6(1): 19-24
Available online at: www.jsirjournal.com

Research Article

ISSN 2320-4818
JSIR 2017; 6(1): 19-24

Received: 15-01-2017
Accepted: 06-02-2017

Muhammad Gul
PhD Scholar, National Center of Excellence in Physical Chemistry, University of Peshawar, Peshawar-25120, Pakistan

Dr. Khalida Akhtar
National Center of Excellence in Physical Chemistry, University of Peshawar, Peshawar-25120, Pakistan

Correspondence:
Muhammad Gul
PhD Scholar, National Center of Excellence in Physical Chemistry, University of Peshawar, Peshawar-25120, Pakistan

Synthesis of magnetic $ZnFe_{1.5}Al_{0.5}O_4$ nanoparticles and their photocatalytic activity testing under sunlight irradiation

Muhammad Gul, Khalida Akhtar*

Abstract

$ZnFe_{1.5}Al_{0.5}O_4$ nanoparticles, uniform in size and shape, were synthesized by coprecipitation method, calcined at 1000 ℃ and were then characterized by scanning electron microscopy, X-ray diffractometery, and Fourier-transform infra-red spectroscopy. Photocatalytic activity of the nanoparticles was tested by dispersing them in Methylene blue solution to attain adsorption-desorption equilibrium and then irradiating with direct sunlight till 1 h. The degradation process was found rapid and the solution became colorless indicating successful removal of the dye. Various radical scavengers were used to identify the species responsible for dye degradation. The adsorbent was easily collected using a permanent magnet and recycled. Comparable results were obtained for reusing the nanoparticles up to 6 cycles. The advantages of effective degradation of dye, magnetic recovery and reusability of $ZnFe_{1.5}Al_{0.5}O_4$ nanoparticles make them a promising material for wastewater treatment.

Keywords: Nanoparticles, Coprecipitation, Photocatalyst, Methylene blue.

INTRODUCTION

Dyeing technology has become one of the basic needs of humans to live in the colourful world. However, synthetic dyes when released into environment become problematic to living organisms due to their slow or even no biodegradability. The aquatic pollution caused by synthetic dyes is a serious environmental issue worldwide.[1] Dyes are densely coloured substances and its trace amount can permit appreciable colour to water. The colouring of water is unwanted because it blocks penetration of sunlight into water, retarding photosynthesis and the growth of aquatic biota is retarded. Moreover, dyes interfere with solubility of gases in water bodies.[2] Therefore, the effluents contaminated with dyes must be treated before their discharge into municipal environments. Untreated effluents are hazardous to aquatic life due to formation of toxic carcinogenic breakdown products. The highest rate of toxicity has been reported for basic and diazo dyes [3,4] and Methylene blue (MB) is one of the basic dyes commonly used in textile industry and for dyeing wooden furniture. Acute exposure to MB is harmful by causing vomiting, nausea, increased heartbeat, cyanosis, jaundice and tissue necrosis in humans[5].

Several methods have been practiced for removal of dyes from waste water such as coagulation and flocculation [6], liquid–liquid extraction [7], chemical oxidation [8], adsorption [5,9] and electrochemical treatment [10]. Due to increasing amount of organic pollutants in water bodies and non-biodegradability of dyes, the conventional methods are becoming less effective. As a consequence, development of a more effective and economical technology for waste water treatment is demanded. Photocatalytic degradation is the best alternative to conventional methods [11] and various photo-catalysts have been developed by researchers.[12,13] Among these, $ZnFe_2O_4$ is practiced by many researchers for dyes degradation because $ZnFe_2O_4$ has narrow band gap (1.9 ev) and non-toxic nature, however, its photocatalytic activity is less due to poor quantum efficiency. Attempts have been made by researchers to overcome this limitation, e.g. Cao et al. loaded Ag on the surface of $ZnFe_2O_4$ but the Ag content was very high.[14] Significant improvement in photocatalytic ability under visible light was observed by Harish *et al*. by doping Al into $ZnFe_2O_4$. [11] They reported that $Zn(FeAl)O_4$ is more active than $ZnFe_2O_4$ to degrade organic dye under sunlight.

In this paper, we report photocatalytic activity of magnetically separable, uniform $ZnFe_{1.5}Al_{0.5}O_4$ nanoparticles synthesized by coprecipitation method. Methylene blue was taken as the model dye in this study and its removal from aqueous solutions was evaluated under ordinary sunlight irradiation.

MATERIALS AND METHODS

Materials

Analytical grade $Zn(NO_3)_2.6H_2O$ (Merck), $Fe(NO_3)_3.9H_2O$ (Scharlau), $Al(NO_3)_3.9H_2O$ (Merck), NH_4OH (BDH, England), Methylene blue dye (Mercck), EDTA (Merck), tert. Butanol (Scharlau), Benzoquinone (Scharlau) and H_2O_2 (Scharlau) were employed without further purification. All solutions were made in de-ionized water.

Synthesis of $ZnFe_{1.5}Al_{0.5}O_4$Nanoparticles

Stoichiometric mixture of aqueous solutions of Zn^{2+}, $Fe^{3+}$and Al^{3+} was heated to 80 ℃ in a double walled cell connected to a water bath (WiseCircu WCB-6) under constant stirring on a magnetic stirrer (WiseStir MSH-20D). Aqueous 3 $mol.L^{-1}$ solution of NH_3 was used to precipitate metal ions from the heated mixture and the precipitates formed were stirred for 3 h at room temperature. The slurry was aged overnight, filtered under vacuum; the precipitates were washed with distilled water and then dried in an electric oven (BINDER FD53) at 100 ℃ for 20 h.

The precipitates obtained were calcined at 1000 ℃ for 2 h in an electric furnace (Nabertherm, L5/11) in air atmosphere which transformed the precipitated non-magnetic metal hydroxide precursors into the magnetic ferrite.

Characterization

Scanning electron microscope (JEOL, JSM-5910) was used to study morphology of the synthesized particles. Crystalline nature and phase of the calcined particles was studied by an X-ray Diffractometer (X'pert PRO, PAN alytical, The Neitherland) with CuKα(λ=1.5406 Å) radiation at step angle 0.02°. FT-IR spectroscopic technique was employed to characterize bond vibrations in the range 4000–400 cm^{-1}. Optical spectrum of the calcined nano-photocatalyst was recorded by visible spectrophotometer (Vernier spectro vis plus, SVIS-PL, Beaverton) in the range 280–800 nm. The residual dye concentration in the solution was determined by UV/Vis spectrophotometer (Spectronic 601) at wavelength of 665 nm.

Photocatalytic study

The synthesized photocatalyst nanoparticles were heated at 100 ℃ for 30 min to eliminate surface adsorbed moisture and other species and then stored in desicator. For photocatalytic activity testing, 5mg nanoparticles were added to20 mL of methylene blue solution with a concentration of 10 $mg.L^{-1}$. The mixture was incubated in dark chamber for 30 min to reach adsorption-desorption equilibrium at ambient temperature. After adding 2 mL (30%) H_2O_2, the suspension was kept under natural sunlight irradaitions with similar conditions on sunny days of April between 11 a.m. and 2 p.m. where fluctuations in the sunlight intensity were insignificant. In this period, the sky was clear and the sunlight was intense in Peshawar (Pakistan). The residual dye concentration in the mixture was monitored by UV/Vis spectrophotometer (Spectronic 601) at regular intervals and the photocatalyst nanoparticles were magnetically separated to be reused for additional runs. The same experiment was repeated in dark and in the absense of either H_2O_2 or catalyst, both in dark and sunlight, to systematically investigate the roll of each parameter.

RESULTS AND DISCUSSION

SEM Analysis

Fig. 1 depicts the scanning electron micrograph (SEM) of synthesized product at different magnifications. It is clear from the micrographs that the synthesized product is composed of elongated nanoparticles which are uniform in size and shape. The average diameter and length of particles were determined to be 58 and 140 nm, respectively. The axial ratio was calculated to be 2.3 for these particles. As the particles are very small, so they get aggregated to certain extent due to high surface-to-volume ratio as well as magnetic interactions.

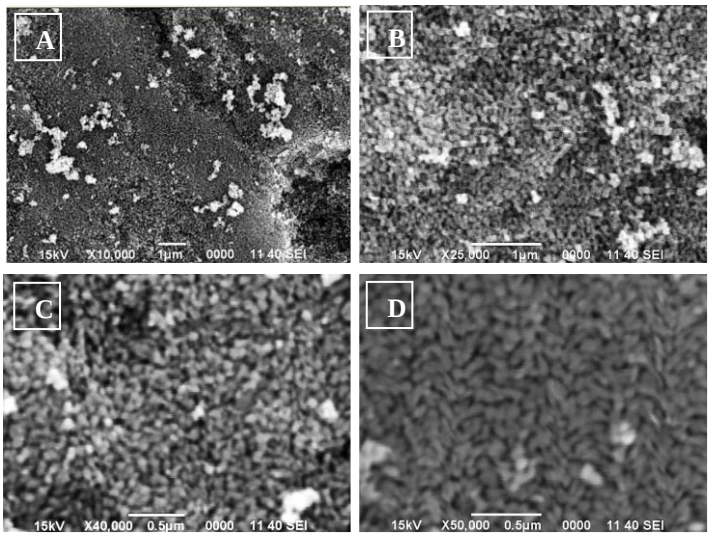

Figure 1: The scanning electron micrograph (SEM) of $ZnFe_{1.5}Al_{0.5}O_4$ nanoparticles, calcined at 1000 ℃ for 2 h in air atmosphere, at different magnifications

Structural Analysis

X-rays diffraction analysis was performed on synthesized particles and the recorded pattern is depicted in Fig. 2. Experimentally determined values of d-spacing, 2θ and the relative intensities of peaks agree with the standard XRD pattern. The diffraction peaks at 2θ 30.61°, 35.91°, 37.4°, 43.65°, 54.25°, 57.78°, and 63.35° are the reflections corresponding to the miller indices (220), (311), (222), (400), (422), (511), and (440), respectively. These diffraction peaks confirm the formation of cubic spinel structure of crystal having space group Fd-3m (PDF ♯ 82-1041). However, the minor impurity phase detected was hematite (PDF ♯ 84-308). The hematite emerged possibly due to evaporation of some amount of Zn at higher temperature. Moreover, the deviation from zero value of ordinate in XRD curve could be indicative of presence of some amorphous content in the sample. Scherer equation (Eq. 1) was used to determine the average crystallite size of the heat treated crystalline materials from the major diffraction peaks for spinel phase.[15]

$$D_p = \frac{0.9\,\lambda}{\beta.\cos\theta} \qquad (1)$$

Where

D= crystallite size

λ = 1.54 Å

β= the line broadening at half maximum intensity (FWHM), and

θ = Bragg's angle

The average crystallite size was found to be 58 nm in the present sample. The lattice parameter 'a', the x-ray density (D_x) and specific surface area (S) of the sample were calculated using Eqs. 2-4, respectively,

$$a = d\sqrt{h^2 + k^2 + l^2} \quad (2)$$

$$D_x = \frac{8M}{Na^3} \quad (3)$$

$$S = \frac{6000}{D_x.D_p} \quad (4)$$

Where, M is molar mass of the sample, N is Avogadro's number, a is the lattice parameter of the sample and 8 represents the number of formula units in the cubic spinel cell.

The lattice parameter was found to be 8.278 nm which is comparable to the standard data (PDF # 82-1041). The value of D_x calculated for $ZnFe_{1.5}Al_{0.5}O_4$ nanoparticles was 5.3 g.cm^{-3} which agrees with the standard data (5.11 g.cm^{-3}). By putting the values of D and D_x in Eq. 4, the specific surface area (S) of particles was found to be 21.34 m^2.g^{-1}.

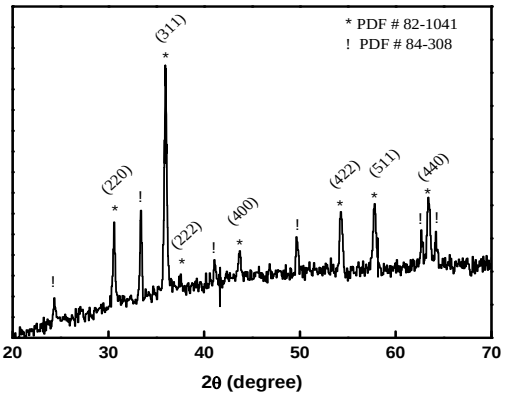

Figure 2: X-ray diffractogram (XRD) of particles shown in Figure 1

FTIR spectroscopy

Fig. 3 depicts the FTIR spectrum of synthesized $ZnFe_{1.5}Al_{0.5}O_4$ nanoparticles. In spinel compounds, the region 1000-200 cm^{-1} is considered important to allocate vibrations of metal ions in the crystal lattice. Two characteristic bands can be observed in this region. The highest one (ϑ_1) occurring in the range 600–500 cm^{-1} corresponds to intrinsic stretching vibrations of the metal at the tetrahedral site (A site), whereas the lower band (ϑ_2) usually observed in the range 450–385 cm^{-1} is assigned to octahedral-metal stretching (B site).[16] Peak appeared around 800-1160 cm^{-1} correspond to the Al-O bond.[17] Interestingly, additional peak at 477 cm^{-1} confirm the existence of secondary hematite phase, as clear from XRD results.[18] The occurrence of absorption bands observed around 3475 and1630 cm^{-1} proved the presence of adsorbed water on the surface of the photocatalyst nanoparticles.[15] The photocatalyst was, therefore, heated at 100 ℃ before use in photocatalytic experiments so as to evaporate the adsorbed water.

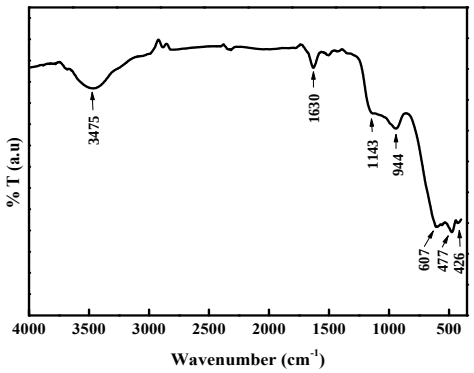

Figure 3: FTIR spectrum of particles shown in Figure 1

Photocatalytic activity test

Photo-degradation being an advanced oxidation process (AOP) degrades the organic pollutants due to its oxidation by highly reactive OH$^{\bullet}$ radicals. These radicals are formed due to electron-hole pair generation when a semiconductor absorbs suitable energy. Here, the photocatalytic efficiency of $ZnFe_{1.5}Al_{0.5}O_4$ nanoparticles was investigated by degrading MB under natural sunlight. The catalyst under study follows Fenton oxidation mechanism, however, the substitution of Al into the $ZnFe_2O_4$ matrix significantly enhance the degradation process by decreasing the band gap and formation of metastable energy levels. These effects of Al substitution into $ZnFe_2O_4$ lead to shift of absorption towards visible region.[11] The photocatalytic mechanism is formulated below (Eqs. 5-7):

$$ZnFe_{1.5}Al_{0.5}O_4 + h\upsilon \rightarrow \bar{e}_{CB} + h^+_{VB} \quad (5)$$

$$(H_2O \leftrightarrow H^+ + OH^-) + h^+_{VB} \rightarrow OH^{\bullet} + H^+ \quad (6)$$

$$OH^{\bullet} + \text{dye} \longrightarrow \text{degradation product} \quad (7)$$

The $ZnFe_{1.5}Al_{0.5}O_4$ nanoparticles absorbs sunlight and create electrons in the conduction band while holes in the valence band. The highly reactive OH$^{\bullet}$ radicals are formed when the hydroxide ions transfer an electron to holes in valence band. Meanwhile, the electrons that are formed can react with the adsorbed molecular oxygen to yield $O_2^{\bullet-}$. The generated $O_2^{\bullet-}$ then further combine with H^+ to produce $HO^{\bullet 2}$, which can react with the electrons to generate OH$^{\bullet}$ radicals. The OH$^{\bullet}$ radicals then oxidize the dye molecules into simple organic moiety. The presence of H_2O_2 significantly enhances the formation of hydroxyl radicals on the surface of nanoparticles under sunlight.[19]

Fig. 4 depicts the optical spectrum of magnetic nano-photocatalyst $ZnFe_{1.5}Al_{0.5}O_4$ in visible region. It is observed that the nanoparticles understudy show maximum absorption between wavelength 380 and 500 nm. The absorption in visible region confirms the usage of synthesized nanoparticles as promising photocatalyst under direct sunlight because 46% fraction of sunlight is visible radiation while only 3% is UV radiation.[11] Therefore, the $ZnFe_{1.5}Al_{0.5}O_4$ are advantageous to properly harvest the solar energy. The enhanced photocatalytic performance due to Al substitution into $ZnFe_2O_4$ has also been reported by Harish *et al.,* however, the concentration of Al^{3+} ions they used was very high. In contrast to Harish *et al.,* in the current study we used lower Al^{3+} content in order to see whether it affect the photocatalytic efficiency of $ZnFe_2O_4$ or not.[11]

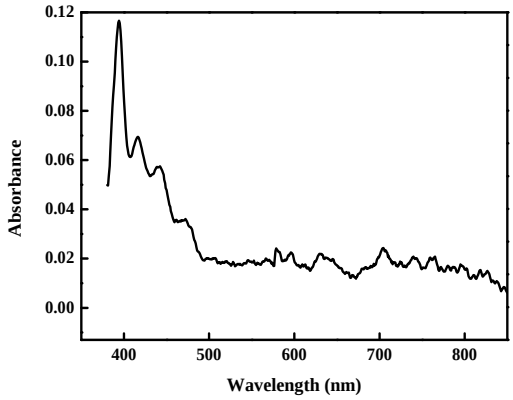

Figure 4: Optical spectra of $ZnFe_{1.5}Al_{0.5}O_4$ particles in visible region

Fig. 5 demonstrate the photocatalytic activity of magnetic nano-photocatalyst $ZnFe_{1.5}Al_{0.5}O_4$ evaluated by degradation of a model organic dye, Methylene blue, in dark and under natural sunlight irradiation. Following the set of experimental conditions, pH = 6 (the natural pH of aqueous dye solution), dye conc. = 10 $mg.L^{-1}$, and nanoparticles dose = 0.25 $mg.L^{-1}$, the effect of some parameters like oxidizing agent, light and photocatalyst was investigated systematically in order to get insight into the mechanism of photocatalytic process. Blank experiments were performed by illuminating the dye solution (with and without oxidant H_2O_2) with sunlight in the absence of catalyst which indicated that the direct photolysis of MB is negligible. Same was the case when either oxidant or photocatalyst was added to dye solution and kept in dark (Fig. 5a). In case of dye-nanoparticles mixture kept in dark and sunlight, it was found that no catalysis take place and the slight decrease in residual dye concentration is due to adsorption process. It can be seen that the C/C_o values are smaller for dye-nanoparticles system kept in dark than that kept in light because the adsorption process is effective in dark. The photocatalytic activity of particles was further confirmed by placing the dye-oxidant-nanoparticles mixture in dark and identical recipe under sunlight. The residual dye content in the mixture kept in dark was significant while that of the sunlight irradiated specimen was almost vanished within 1 h. It can be concluded from the results displayed in Fig. 5b that the synthesized product is active under natural sunlight. The sunlight irradiation on the surface of nanoparticles induces the free radical formation by transfer of electron from surface adsorbed H_2O or OH^- into the hole in valance band of $ZnFe_{1.5}Al_{0.5}O_4$. The oxidant H_2O_2 act as an effective electron scavenger to form $OH^{\bullet}$ radical on the surface of $ZnFe_{1.5}Al_{0.5}O_4$ nanoparticles. That is why effective degradation of MB is observed in the presence of H_2O_2 under direct sunlight irradiation. It is worth mentioning that Harish *et al.* observed degradation of methylene blue dye with $ZnFeAlO_4$ under sunlight in 4 h for 10 $mg.L^{-1}$ initial concentration of dye.[11]

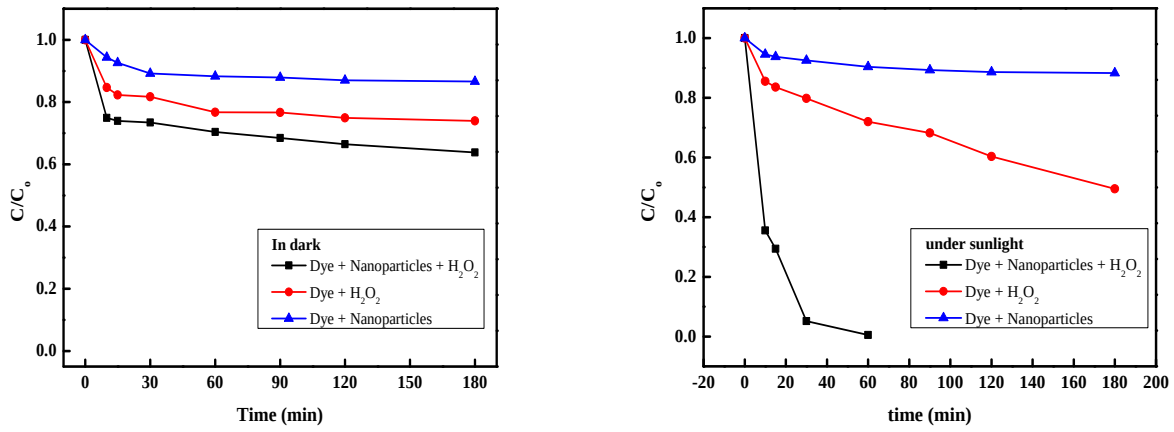

Figure 5: Degradation curves of methylene blue monitored as the normalized concentration change vs time using series samples (A) in dark and (B) under sunlight irradiation

The Langmuir-Hinshelwood model was used to describe the kinetics of the process, which may be expressed by $\ln(C_0/C) = Kt$ for relatively lower concentration of dye (where C_0 shows the initial concentration of dye, C is the residual dye concentration at time "t", and K denotes the apparent first order rate constant). The plot of $\ln(C_0/C)$ vs t (Fig. 6) gives the value of K. The rate constant is an important parameter which is used as an assessment index for evaluating the photocatalytic efficiency of synthesized materials. It is worth mentioning that the kinetic plot for the synthesized catalyst is almost linear and the obtained values of apparent rate constant "K" obtained at various experimental conditions are listed in Table 1.

To probe the active species in the degradation process, 5 mL of EDTA (0.01 $mol.L^{-1}$), tert-butanol (t-BuOH, 0.5 $mol.L^{-1}$), and benzoquinone (BQ, 1 $mol.L^{-1}$) were separately added to the reaction mixture (Fig. 5b, Dye+Nanoparticles+H_2O_2) and kept under sunlight with identical experimental conditions. It was observed that the addition of $OH^{\bullet}$ scavenger, t-BuOH, and EDTA, into the system lead to decreased degradation rate of MB. Contrarily, the addition of O^{2-} scavenger (BQ) to the system showed no significant effect on the degradation rate of MB, indicating that the O^{2-} is not a major oxidizing species. These results emphasize that $OH^{\bullet}$ species are responsible for carrying out photo-oxidation reaction. Therefore, the photocatalytic reaction could continue through a direct hole and the electron transfer process.

Table 1: Methylene blue degradation efficiency of $ZnFe_{1.5}Al_{0.5}O_4$ nanoparticles and their apparent first order rate constants

S. No.	Recipe	%-age decrease in dye conc. in 1 h	K (min^{-1})
1	Dye + Nanoparticles + H_2O_2	99.46	8.745×10^{-2}
2	Dye + H_2O_2	28	3.4×10^{-3}
3	Dye + Nanoparticles	9.62	5.50×10^{-4}

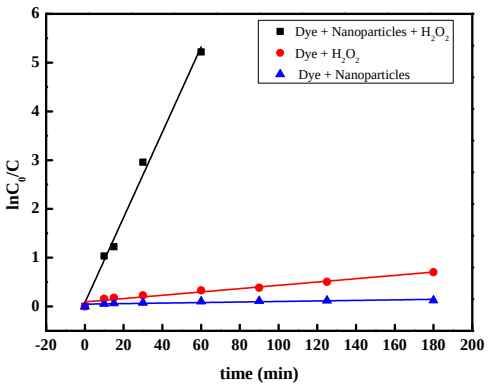

Figure 6: Kinetic plots for apparent rate constant for MB dye degradation under sunlight irradiation at different experimental conditions

Recovery of catalyst

The magnetic property of the $ZnFe_{1.5}Al_{0.5}O_4$ nanoparticles is advantageous for efficient recovery of magnetic photocatalysts in liquid-phase reactions. The photocatalyst was successfully collected by applying a permanent magnet along the wall of reaction vessel, as shown in Fig. 7(C). Before reuse, they were dispersed in ethanol to desorb the surface adsorbed MB molecules if any. However, the MB concentration was found negligible in ethanol which point towards the degradation as dominant process in dye removal by $ZnFe_{1.5}Al_{0.5}O_4$ nanoparticles.

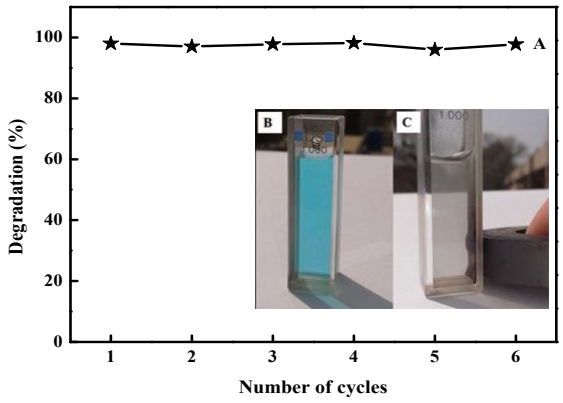

Figure 7: (A) The photodegradation percent of MB dye in solution for 6 cycles using $ZnFe_{1.5}Al_{0.5}O_4$ nanophotocatalyst under sunlight irradiation. The inset shows the photographs of MB solution (B) before adsorption and (C) after degradation by $ZnFe_{1.5}Al_{0.5}O_4$ nanoparticles. The magnetic $ZnFe_{1.5}Al_{0.5}O_4$ nanophotocatalyst is separable by applying permanent magnet outside the wall of the container

Recyclability of catalyst

The recycling ability of the $ZnFe_{1.5}Al_{0.5}O_4$ nanoparticles was explored by conducting recycling experiments. The performance of the particles recycled for 6 cycles with identical experimental conditions is demonstrated in Fig. 7(A). It is observed that photocatalytic ability is not affected in 6 cycles which proved that the synthesized nanoparticles are highly stable, magnetically separable and recyclable and can be used as an efficient photoactive catalyst for degradation of organic pollutants.

CONCLUSIONS

$ZnFe_{1.5}Al_{0.5}O_4$ nanoparticles, uniform in size and morphology, were synthesized via controlled chemical coprecipitation route and then characterized for morphological, structural, optical and functional group analysis. XRD analysis revealed the formation of spinel ferrite phase ($ZnFe_{1.5}Al_{0.5}O_4$) with traces of secondary hematite phase. The same was confirmed by FTIR spectroscopy. Optical spectrum showed that the synthesized nanoparticles do absorb in visible region (380-500 nm). The photocatalytic activity of particles was tested for methylene blue under direct sunlight and almost complete degradation of dye on the surface of nano-photocatalyst was achieved with in 1h in the presence of H_2O_2 and sunlight. Use of $OH^{\bullet}$ radicals and O^{2-} scavengers confirmed that $OH^{\bullet}$ radicals are playing the major role in degradation of dye. The nanoparticles were easily recovered by simply putting a permanent magnet across the wall of the container. Recycling experiments showed negligible change in the efficiency of the synthesized product till 6 runs under identical conditions. The effective degradation of dye, magnetic separation, and recycling efficiency make $ZnFe_{1.5}Al_{0.5}O_4$ nanoparticles an outstanding candidate material for water treatment and purification.

Acknowledgement

National Centre of Excellence in Physical Chemistry, University of Peshawar, Peshawar-25120, Khyber Pakhtunkhwa, Pakistan is highly acknowledged to facilitate this research work.

No conflict of interest: Nil

REFERENCES

1. Ainane, T.; Khammour, F.; Talbi, M., A novel bio-adsorbent of mint waste for dyes remediation in aqueous environments: study and modeling of isotherms for removal of methylene Blue. Oriental Journal of Chemistry 2014,30 (3), 1183-1189.
2. Garg, V. K.; Amita, M.; Kumar, R.; Gupta, R., Basic dye (methylene blue) removal from simulated wastewater by adsorption using Indian Rosewood sawdust: a timber industry waste. Dyes and pigments 2004,63 (3), 243-250.
3. Lata, H.; Garg, V.; Gupta, R., Removal of a basic dye from aqueous solution by adsorption using Parthenium hysterophorus: an agricultural waste. Dyes and pigments 2007,74 (3), 653-658.
4. Wang, X. S.; Zhou, Y.; Jiang, Y.; Sun, C., The removal of basic dyes from aqueous solutions using agricultural by-products. Journal of Hazardous Materials 2008,157 (2), 374-385.
5. Shahryari, Z.; Goharrizi, A. S.; Azadi, M., Experimental study of methylene blue adsorption from aqueous solutions onto carbon nano tubes. Int J Water Res Environ Eng 2010,2 (2), 16-28.
6. Kim, T.-H.; Park, C.; Yang, J.; Kim, S., Comparison of disperse and reactive dye removals by chemical coagulation and Fenton oxidation. Journal of Hazardous Materials 2004,112 (1), 95-103.
7. Muthuraman, G.; Teng, T. T.; Leh, C. P.; Norli, I., Extraction and recovery of methylene blue from industrial wastewater using benzoic acid as an extractant. Journal of Hazardous Materials 2009,163 (1), 363-369.
8. Dutta, K.; Mukhopadhyay, S.; Bhattacharjee, S.; Chaudhuri, B., Chemical oxidation of methylene blue using a Fenton-like reaction. Journal of Hazardous Materials 2001,84 (1), 57-71.
9. Rafatullah, M.; Sulaiman, O.; Hashim, R.; Ahmad, A., Adsorption of methylene blue on low-cost adsorbents: a review. Journal of Hazardous Materials 2010,177 (1), 70-80.
10. Panizza, M.; Barbucci, A.; Ricotti, R.; Cerisola, G., Electrochemical degradation of methylene blue. Separation and purification technology 2007,54 (3), 382-387.
11. Harish, K.; Bhojya Naik, H., Solar light active ZnFe2-xAlxO4 materials for optical and photocatalytic activity: an efficient photocatalyst. International Journal of Science Research 2013,1 (4), 301-307.
12. Chong, M. N.; Jin, B.; Chow, C. W.; Saint, C., Recent developments in photocatalytic water treatment technology: a review. Water research 2010,44 (10), 2997-3027.
13. Herrmann, J.-M.; Guillard, C.; Pichat, P., Heterogeneous photocatalysis: an emerging technology for water treatment. Catalysis Today 1993,17 (1), 7-20.
14. Cao, X.; Gu, L.; Lan, X.; Zhao, C.; Yao, D.; Sheng, W., Spinel $ZnFe_2O_4$ nanoplates embedded with Ag clusters: preparation, characterization, and

photocatalytic application. Materials Chemistry and Physics 2007,106 (2), 175-180.
15. Gul, M., Radio frequency abnormal dielectric response of manganese chromite ($MnCr_2O_4$) nanoparticles synthesized by coprecipitation method. Materials Research Bulletin 2016,76, 431-435.
16. Allen, G. C.; Paul, M., Chemical characterization of transition metal spinel-type oxides by infrared spectroscopy. Applied spectroscopy 1995,49 (4), 451-458.
17. Parida, K.; Pradhan, A. C.; Das, J.; Sahu, N., Synthesis and characterization of nano-sized porous gamma-alumina by control precipitation method. Materials Chemistry and Physics 2009,113 (1), 244-248.
18. Ellid, M.; Murayed, Y.; Zoto, M.; Musić, S.; Popović, S., Chemical reduction of hematite with starch. Journal of radioanalytical and nuclear chemistry 2003,258 (2), 299-305.
19. Chen, C.-H.; Liang, Y.-H.; Zhang, W.-D., $ZnFe_2O_4$/MWCNTs composite with enhanced photocatalytic activity under visible-light irradiation. Journal of Alloys and Compounds 2010,501 (1), 168-172.